Int. J. Heat Mass Transfer. Vol. 23, pp. 1219–1228
Pergamon Press Ltd. 1980. Printed in Great Britain

THERMOELECTRIC MHD WITH WALLS PARALLEL TO THE MAGNETIC FIELD

J. A. SHERCLIFF
Department of Engineering, University of Warwick, Coventry, CV4 7AL, U.K.

(*Received* 21 *November* 1979)

Abstract—Liquid metal within metal walls under a magnetic field is stirred thermoelectrically if the interfacial temperature is non-uniform. When there are areas of interface parallel to the uniform magnetic field, fast boundary layers occur, exchanging fluid with the central region. Outside these layers, viscosity and inertia may be neglected if the magnetic field is strong. Motions in long ducts of rectangular cross-section, closed cylinders coaxial with the field, and cubical containers are investigated. As the interface temperature is assumed to be known *ab initio*, the strong effects of heat convection are not explored.

NOMENCLATURE

$\mathbf{B}, B$,	magnetic field;
C,	$a\sigma/t\sigma_w$, $C' = b\sigma/t\sigma_w$;
$\mathscr{E}$,	Seebeck emf;
G,	$W + B\psi$;
H,	current stream function;
M,	$Ba(\sigma/\eta)^{1/2}$, Hartmann number;
Q_s, Q_x, Q_y, Q_z,	components of boundary layer flow integral;
$S(S_w)$,	absolute thermoelectric power of fluid (wall);
T,	$\tanh(na/b)$ (or temperature);
U,	pseudo-potential in wall parallel to $\mathbf{B}$;
V,	pseudo-potential in wall normal to $\mathbf{B}$;
W,	pseudo-potential in fluid;
a,	semiwidth of duct or container;
b,	cylinder radius or duct height;
c,	$C^{1/2}/a$;
h,	mesh step size;
$\mathbf{j}, j$,	current intensity;
$\mathbf{j}'$,	current intensity in planes z = const.;
m,	number of mesh steps;
n,	normal distance (see Fig. 1);
p,	fluid pressure;
s,	tangential distance (see Fig. 1);
t,	wall thickness;
$\mathbf{v}, v$,	velocity.

Greek symbols

$\sigma(\sigma_w)$,	electrical conductivity of fluid (wall), assumed constant;
η,	viscosity;
ψ,	stream function.

1. INTRODUCTION

UNDER an imposed magnetic field, thermoelectric currents cause stirring of a liquid metal in a metal container when the interface temperature is non-uniform. Such a phenomenon could have relevance to controlled fusion or metallurgical technology. For instance, for liquid lithium cells in the blanket of a magnetically-confined fusion reactor, heated by neutrons and cooled by helium circulation, temperature distributions calculated on the assumption of static fluid could be grossly in error because of the stirring (lithium has unusually high thermoelectric power). Similarly, the possibility of achieving desirable stirring during the solidification of melts in metallurgy is worthy of investigation.

This paper extends earlier studies [1–3], of which [1] discussed the size of the effect in practice and analysed motions in long circular ducts, whereas [2] and [3] examined TEMHD in closed containers. [1] and [2] specifically excluded cases where finite portions of the interface are parallel to the magnetic field but [3] considered circular pipes of finite length closed by plane ends parallel to the field. This paper explores other problems where some walls are parallel to the field, the other two walls being plane and normal to the uniform imposed magnetic field. The problems are specified in terms of known distributions of temperature and hence of Seebeck emf over the wall–fluid interface; at this early stage in the subject there is quite enough complication without having to explore the perturbation of the heat supply necessary to maintain these temperatures in the face of the convection which ensues when the magnetic field is applied. The effect can be quite severe because significant Peclét numbers can occur [2].

In practice, any magnetic field due to the currents is negligible and inertia forces are usually insignificant in comparison with magnetic forces. Each problem is then linear and appropriate solutions may be conveniently superposed. As the Hartmann number M is large, there are boundary layers on walls parallel to the field of thickness $O(M^{-1/2})$ (if laminar) and Hartmann layers of thickness $O(M^{-1})$ on the other walls, while the core flow elsewhere is inviscid. The importance of wall impedance is measured by the parameter C and is small compared with boundary-layer impedance because C is normally small compared with M and $M^{1/2}$. Then the Hartmann layers are entirely negligible but

the fluid in the layers parallel to the field may travel so fast that they can carry significant flow and 'hold off' significant potential drops by electromagnetic induction, as [3] showed. It is possible to proceed without solving for their structure in detail and so it is not necessary to neglect inertia in those layers (which might even be turbulent) provided they are still thin. In the container problems solved here the flow passes between the core and the high-speed layers.

We take the walls to be thin ($t \ll a$) in order to treat wall current flow as quasi-two-dimensional and to ignore the fine structure of current flow round corners in the walls. We take the z-axis in the direction of the magnetic field and the y-axis axial in duct flow problems. The plane walls normal to the field are at $z = +a$, as in Fig. 1.

In view of the dependency of the heat convection on the vigour of the stirring process, some attention is given to those extreme cases in which either there is no motion or there is 'free' motion, where the fluid can accelerate until $\mathbf{v} \times \mathbf{B}$ and Seebeck emf's balance and currents cease.

2. GOVERNING EQUATIONS

In the inviscid, inertia-free core, the $\mathbf{j} \times \mathbf{B}$ force balances the pressure gradient and is therefore irrotational, so that $\mathbf{j}$ is independent of z and

$$\operatorname{div} \mathbf{j}' = 0, \tag{1}$$

$\mathbf{j}'$ being the current intensity in planes $z = \text{const.}$ Ohm's law in TEMHD is

$$\mathbf{j}/\sigma = \mathbf{v} \times \mathbf{B} - \operatorname{grad} W \tag{2}$$

in which

$$W = \text{electric potential} + \int_{T_0} S \, dT, \tag{3}$$

T_0 being a datum temperature. We replace W by V or U respectively in walls normal or parallel to $\mathbf{B}$. At the interface

$$W = V \text{ (or } U) + \mathscr{E}, \tag{4}$$

where the Seebeck emf $\mathscr{E} = \int_{T_0} (S - S_w) dT$, a function of the interface temperature. At the high-speed layers, W in (4) must be taken at the wall proper, not the edge of the core. The curl of (2) in the fluid makes $\mathbf{v}$ linear in z if we take the fluid as incompressible, with

$$\operatorname{div} \mathbf{v} = 0. \tag{5}$$

As the Hartmann layers are thin and move at slow speed, v_z vanishes at the walls $z = \pm a$ and, being linear in z, vanishes throughout the core. From (5) we may then set

$$v_x = \partial\psi/\partial y \quad \text{and} \quad v_y = -\partial\psi/\partial x \tag{6}$$

and (2) allows us to take $G = W + B\psi$ as independent of z, with

$$\mathbf{j}' = -\sigma \operatorname{grad} G \tag{7}$$

and

$$\nabla^2 G = 0, \tag{8}$$

in view of (1). At the walls parallel to $\mathbf{B}$, the high impedance layers have negligible effect on the normal component of $\mathbf{j}'$, which may be taken as equal to the value at the edge of the core.

Although in the core $v_z = 0$, this is not true in general in the layers parallel to $\mathbf{B}$, across which we define two flow integrals

$$Q_s = \int v_s \, dn \quad \text{and} \quad Q_z = \int v_z \, dn. \tag{9}$$

Neglect of the current term in integrating (4) leads to the condition

$$BQ_s = U + \mathscr{E} - W \tag{10}$$

in which W is the value at the edge of the core. Equation (10) expresses the 'holding off' of p.d. by the high-speed layer. Q_s vanishes at the rims where $\mathscr{E}$ is assumed continuous and where we have the further conditions

$$V = U \quad \text{and} \quad \partial U/\partial z = \pm \partial V/\partial n \text{ (as appropriate).} \tag{11}$$

(For simplicity we take all walls as having the same thickness and conductivity.) Fluid conservation at the layers requires that

$$\frac{\partial Q_s}{\partial s} + \frac{\partial Q_z}{\partial z} = \frac{\partial \psi}{\partial s} \text{ or } B\frac{\partial Q_z}{\partial z} = \frac{\partial}{\partial s}(G - U - \mathscr{E}) \tag{12}$$

by virtue of (10). Q_z also vanishes at the rims, for the Hartmann layers cannot accommodate significant flows. Equation (12) may therefore be integrated from $z = -a$, say, to yield Q_z.

In view of the symmetry in the plane $z = 0$, it is convenient to follow [2] and [3] in considering solutions for $\mathscr{E}$ odd or even with respect to z separately and then superposing them, as necessary.

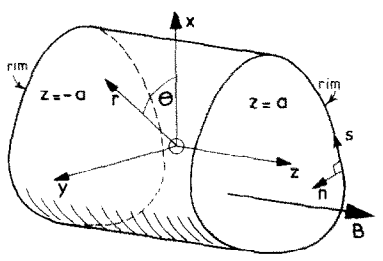

FIG. 1. TEMHD container.

2.1. $\mathscr{E}$ Even in z

For the case where $\mathscr{E}$ is even, [2] showed that in the core $j_z = 0$ while W, G and ψ are independent of z. In the walls

$$\frac{\partial^2 V}{\partial x^2} + \frac{\partial^2 V}{\partial y^2} = 0 \tag{13}$$

and

$$\frac{\partial^2 U}{\partial s^2} + \frac{\partial^2 U}{\partial z^2} = -\frac{C}{a}\frac{\partial G}{\partial n}. \tag{14}$$

By (8) and (13), the core vorticity is given by

$$-\nabla^2\psi = \nabla^2\mathscr{E}/B, \tag{15}$$

$\mathscr{E}$ being the value at the faces $z = \pm a$. The vanishing of the vorticity does not preclude motion as all streamlines may enter and leave the boundary layers. As j_z and v_z vanish, half of these $\mathscr{E}$-even solutions (e.g. for $z > 0$) may be taken to represent a system having one plane wall normal to the magnetic field non-conducting (or a horizontal free surface taken to be virtually plane) at $z = 0$. Here Q_z is odd in z and zero at $z = 0$ also. Integrating (12) from $z = 0$ to a and also with respect to s gives a boundary condition for G, namely

$$\bar{U} + \bar{\mathscr{E}} = G_{\text{rim}} + \text{constant}, \tag{16}$$

in which $\bar{U}$ and $\bar{\mathscr{E}}$ are mean values with respect to z in or at the walls parallel to **B**. We see that G, V, U and the wall and core currents depend only on $\bar{\mathscr{E}}$, and not on the detail distribution of $\mathscr{E}$, but the core *motion* also depends on $\mathscr{E}$ on the walls *normal* to **B** according to the equation

$$B\psi = G - V - \mathscr{E}. \tag{17}$$

Q_s is determined purely by $\mathscr{E}$ on the walls parallel to **B**, by the relation

$$BQ_s = U + \mathscr{E} - U_{\text{rim}} - \mathscr{E}_{\text{rim}}, \tag{18}$$

which shows that Q_s can be made zero everywhere by a suitable choice of $\mathscr{E}$ on the walls parallel to **B**. Then $Q_z = 0$ also and $\psi_{\text{rim}} = \text{const}$, as the core flow cannot feed the layers.

2.2. $\mathscr{E}$ *Odd in* z

For the case where $\mathscr{E}$ is odd, [2] showed that in the core the only current component is j_z, which is independent of z, but W, ψ, v_x, v_y are proportional to z. In fact, in the core,

$$B\psi = zj_z/\sigma = -W \tag{19}$$

while, in the walls,

$$\frac{\partial^2 V}{\partial x^2} + \frac{\partial^2 V}{\partial y^2} = \frac{C(V + \mathscr{E})}{a^2} \tag{20}$$

and

$$\frac{\partial^2 U}{\partial s^2} + \frac{\partial^2 U}{\partial z^2} = 0. \tag{21}$$

A condition such as (16) is neither necessary nor available. The values of V, U, ψ and j_z are fixed purely by $\mathscr{E}$ at $z = \pm a$; $\mathscr{E}$ on the walls parallel to **B** has no effect on the core; variations in $\mathscr{E}$ there affect only the boundary layers, via (10). Because ψ is odd in z, fluid enters and leaves the layers on opposite sides of $z = 0$, where Q_z is not zero so that return flow in the layers across $z = 0$ is possible. Q_z is determined by (12) with $G = 0$. A simple case is that where $\mathscr{E}$ is such that Q_s is zero everywhere and Q_z is proportional to $(a^2 - z^2)$.

2.3. *Current-free cases*

A first task is to establish whether the fluid can ever accelerate until all currents vanish (to the order of this calculation) because the $\mathbf{v} \times \mathbf{B}$ and Seebeck emf's balance. Then the thickness and conductivity of the current-free walls become immaterial (provided $C \ll M^{1/2}$) and V and U are uniform. G is uniform by (7) and so $B\psi + \mathscr{E} = \text{const}$. at the walls $z = \pm a$. $\mathscr{E}$ must be even in z as $j_z = 0$. The streamlines and side-wall isotherms are identical. On the other walls $\bar{\mathscr{E}}$ must be independent of s, by (16). There are high-speed boundary layers if $\mathscr{E}$ varies from its value at the rims for (18) here becomes

$$BQ_s = \mathscr{E} - \mathscr{E}_{\text{rim}}. \tag{22}$$

If $\mathscr{E}_{\text{rim}}$ is constant, $\bar{Q}_s$ is constant, $\partial\psi/\partial s$ vanishes and the layer does not drain or feed the core flow. Q_z occurs if $\mathscr{E}$ varies with s. If $\bar{\mathscr{E}}$ varies with s, the problem belongs to the wider category, with core and wall currents, discussed below.

Once there is current in the core and walls, a general treatment for arbitrary cross-sections in the x–y plane becomes cumbersome. Henceforth we therefore consider only the more symmetric configurations in order to reveal the physics without excessive mathematical complication.

3. FULLY DEVELOPED FLOW IN A RECTANGULAR DUCT

In the two-dimensional problem we take the walls parallel to **B** as $x = \pm b$ (see Fig. 2). Currents circulate in x–z planes and the purely axial motion involves no exchange between core and layers. The neglect of inertia in the core is exact here. There may be net axial flow and/or a uniform axial pressure gradient $\mathrm{d}p/\mathrm{d}y$. As in [1] the solution consists of two superposable parts:

1. thermoelectrically-driven motion in the absence of $\mathrm{d}p/\mathrm{d}y$, and
2. isothermal flow due to the pressure gradient.

Although the latter is a well-explored field, the case of

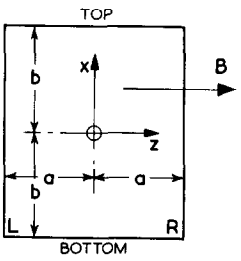

FIG. 2. Duct cross-section.

thin, finitely conducting walls has not been fully covered previously. Now j_z depends only on x, while

$$j_x = -(\mathrm{d}p/\mathrm{d}y)/B, \text{ constant.} \tag{23}$$

3.1. *The boundary layers on walls parallel to* **B**

In relation to these, it is convenient to treat the odd and even parts of the solution together. In the bottom wall (see Fig. 2)

$$\mathrm{d}^2U/\mathrm{d}z^2 = j_x/t\sigma_w, \tag{24}$$

If subscripts L and R refer to the corners indicated, (24) integrates to

$$U = -\tfrac{1}{2}j_x(a^2 - z^2)/t\sigma_w + \{(W_R - \mathscr{E}_R)(a + z) + (W_L - \mathscr{E}_L)(a - z)\}/2a.$$

Q_y, which is $\int v_y\,\mathrm{d}n$, is given by (10) as

$$BQ_y = \tfrac{1}{2}j_x(a^2 - z^2)/t\sigma_w + (\mathscr{E}_R - \mathscr{E}_L)z/2a + \tfrac{1}{2}(\mathscr{E}_R + \mathscr{E}_L) - \bar{\mathscr{E}} \tag{25}$$

because W at the bottom of the core is linear in z. The high values of v_y enable $\mathbf{v} \times \mathbf{B}$ emf's to hold off both the Seebeck emf's and the pd's due to the spreading of j_x into the wall. Integrating (25) between $z = \pm a$ gives the total flow in the layer, namely

$$\{2a^3j_x/3t\sigma_w + 2a[\tfrac{1}{2}(\mathscr{E}_R + \mathscr{E}_L) - \bar{\mathscr{E}}]\}/B. \tag{26}$$

At the top layer the sign of the thermoelectric term in (26) must be changed. According to the model used here, the part due to pressure gradient becomes zero when $\sigma_w \to \infty$. In a rectangular duct with perfectly conducting walls [4], the velocities in the top and bottom layers are of the same order as the core velocity and BQ_y produces exactly as much emf as would the uniform core velocity, i.e. just enough to drive j_x, as there is no pd across the layer in this case.

In relation to the core, it is convenient to treat odd and even parts separately.

3.2. $\mathscr{E}$ *Odd in* z

When $\mathscr{E}$ is odd, V is determined by (20) in the form

$$\frac{1}{c^2}\frac{\mathrm{d}^2V}{\mathrm{d}x^2} - V = \mathscr{E} \quad (c = C^{1/2}/a) \tag{27}$$

subject to the conditions

$$\frac{\mathrm{d}V}{\mathrm{d}x} = \pm\frac{V}{a} \quad \text{at } z = a, \quad x = \mp B, \tag{28}$$

which arise because U is linear in z by (21). The velocity is given by

$$v_y = \frac{z}{Ba}\frac{\mathrm{d}}{\mathrm{d}x}(V + \mathscr{E}) \tag{29}$$

using the values of V and $\mathscr{E}$ at $z = a$. A solution of (27) usually involves a hyperbolic complementary function, which equals $(V + \mathscr{E})$ in cases where $\mathscr{E}$ at $z = a$ is linear in x (or constant). In fact, if $\mathscr{E} = ka$ (constant) at $z = a$, then in the core

$$v_y = \frac{kz}{B}\frac{c\sinh cx}{ac\sinh cb + \cosh cb} \tag{30}$$

whereas, if $\mathscr{E} = kx$ at $z = a$,

$$v_y = \frac{k(a + b)z}{aB}\frac{c\cosh cx}{ac\cosh cb + \sinh cb}. \tag{31}$$

More generally, if $\mathscr{E}$ at $z = a$ is expressed as a Fourier series in x, (27) is easily solved, but there are also simple polynomial solutions for which

$$V + \mathscr{E} = \Sigma k_m x^{m-2} \ (m \text{ even}) \tag{32}$$

provided that $\mathscr{E}$ (at $z = a$) is the even function

$$\mathscr{E} = \Sigma k_m\{x^{m-2} + C(b^m - x^m + mab^{m-1})/m(m-1)a^2\}. \tag{33}$$

The case $m = 2$ is the only situation for which, with $\mathscr{E}$ odd in z, j_z is constant and v_y is zero. It is referred to again, below.

3.3. $\mathscr{E}$ *Even in* z

When $\mathscr{E}$ is even, $j_z = 0$ and W is independent of z. Conservation of current flow in walls and core across planes x = constant determines the core velocity (a function of x) as

$$v_y = \{j_x(C + 1)/\sigma + \mathrm{d}\mathscr{E}/\mathrm{d}x\}/B, \tag{34}$$

exactly as for circular ducts [1], $\mathscr{E}$ being the value at both side walls at the same x.

Setting the pressure gradient (and j_x) to zero leaves only the current-free solution with $\mathbf{v} \times \mathbf{B}$ and Seebeck emf's in balance. In this case, the total volumetric flow due only to thermoelectric effects, including both the contribution of the boundary layers (26) and the integral of (34), is equal merely to

$$2a(\bar{\mathscr{E}}_T - \bar{\mathscr{E}}_B)/B, \tag{35}$$

if subscripts T and B refer to the top and bottom walls respectively. Equation (35) involves neither the value of C nor the detailed distribution of $\mathscr{E}$. Nor does any *odd* part of $\mathscr{E}$ contribute to the total flow rate.

In the isothermal case, pressure gradient alone produces a flow of

$$\frac{4a}{\sigma B^2}\left(-\frac{\mathrm{d}p}{\mathrm{d}y}\right)\left((C + 1)b + \frac{1}{3}Ca\right), \tag{36}$$

in which the two terms relate to the core and layers respectively and are of the same order unless a/b is very large or small or C is very small.

If thermoelectrically-driven flow is blocked (e.g. by remote ends), superposing (35) and (36) so as to give zero net flow determines the 'standstill' pressure gradient

$$\frac{\mathrm{d}p}{\mathrm{d}y} = \frac{\tfrac{1}{2}\sigma B(\bar{\mathscr{E}}_T - \bar{\mathscr{E}}_B)}{(C + 1)b + \frac{1}{3}Ca}. \tag{37}$$

This case belongs to the class of closed-container problems, treated later. As in [1], the question arises as

to whether the fluid can ever be at rest *everywhere*. For the core to be at rest, (34) indicates that $\mathscr{E}$ (or its even part) at $z = a$ must obey

$$\frac{\mathrm{d}\mathscr{E}}{\mathrm{d}x} = \frac{(C+1)}{\sigma B}\left(\frac{\mathrm{d}p}{\mathrm{d}y}\right) \tag{38}$$

with $\mathrm{d}p/\mathrm{d}y$ given by (37). If $\mathscr{E}$ has an odd part it must be given by (33) with $m = 2$. For the *local* flow Q_y in each layer to be zero, as well, $\mathscr{E}_B$ or $\mathscr{E}_T$ must vary quadratically with z so that (25) vanishes. Then the electrical and mechanical conditions at top and bottom of the core are directly compatible with the walls and no layers occur, i.e. the fluid is stationary everywhere. Then it is not even necessary for M to be large and the magnetic field can be in any direction. $\mathscr{E}$ varies quadratically along each wall so as suitably to cause redistribution of the uniform currents entering obliquely from the fluid.

The case where the top and bottom walls are nonconducting [4] is very different. Then a pressure gradient drives velocities of order M in the layers near these walls and produces a flow rate of order $M^{1/2}$. As a result, blocking the ends of such a duct when the side walls are thermoelectrically active produces a negligible [i.e. $O(M^{-1/2})$] change in the core flow as compared with the free flow without pressure gradient because the boundary layers provide such an easy return path for fluid where j_x and the $\mathbf{j} \times \mathbf{B}$ force necessarily fall to zero. Some indication of how conditions are modified near plane ends on a rectangular duct is given in Section 5, which examines a cubical closed container.

4. CYLINDRICAL CONTAINERS

We turn next to the case where the wall parallel to the field is the cylinder $r = b$, in terms of polar coordinates (r, θ) in x, y planes. This case should be distinguished from that of the circular pipe with plane ends [3], where the field is normal, not parallel, to the axis. The distributions of temperature and $\mathscr{E}$ need not be symmetric about the z-axis and so this case should be reasonably representative of the physical behaviour that occurs with arbitrary smooth cross-sections in x, y planes.

It is fruitful to split $\mathscr{E}$ and the related solutions of this linear problem into Fourier harmonics with respect to θ, which may be superposed. We therefore take

$$(V, G, U, \psi, \mathscr{E}) = (V', G', U', \psi', \mathscr{E}')\cos n\theta$$

referred to a suitable θ-datum for each harmonic, where n is an integer or zero and $\mathscr{E}'$ etc. are functions of z and/or r, as appropriate, and are finite whenever $r = 0$. We consider the solutions for $\mathscr{E}$ even and odd in z separately.

4.1. $\mathscr{E}$ *Even in* z

The axisymmetric part of the core solution (the $n = 0$ harmonic) belongs to the current-free class, with $\mathscr{E}_{z=a} + B\psi = \text{const.}$, i.e. pure swirl, independent of z. $\mathscr{E}$ proportional to r^2 gives solid-body rotation, while $\mathscr{E}$ uniform at $z = \pm a$ leaves the core at rest. The purely swirling ($Q_z = 0$) layer on the curved walls is a high-speed closed circulation, not involving the core, but $Q_s = 0$ (to the order of this calculation) if $\mathscr{E}$ on the curved walls is independent of z, U being zero here.

If $n \neq 0$ the situation is more interesting. V and G are both Laplacian and we may take V' and G' as $A(r/b)^n$ and $D(r/b)^n$ respectively. Then (11) indicates that at the rim $z = a$

$$\frac{b\,\mathrm{d}U'}{\mathrm{d}z} = -nU', \tag{39}$$

while (14) gives

$$\frac{\mathrm{d}^2U'}{\mathrm{d}z^2} - \frac{n^2U'}{b^2} = \frac{nCD}{ab} \tag{40}$$

from which

$$U' = E\cosh(nz/b)/\cosh(na/b) - CDb/na. \tag{41}$$

This satisfies (39) and (11) if

$$D = En(1+T)/C' \quad \text{and} \quad A = -ET \tag{42}$$

in which C' denotes $b\sigma/t\sigma_w$ and $T = \tanh(na/b)$. Equation (16) then fixes E as

$$E = \bar{\mathscr{E}}'/((1 + n/C')(1+T) - bT/na), \tag{43}$$

where $\bar{\mathscr{E}}'$ is the mean value of $\mathscr{E}'$ with respect to z on the curved walls, which suffices to determine the U, V and current distributions. However the distribution of $\mathscr{E}$ on the walls $z = \pm a$ affects the motion via (17) which gives

$$B\psi' = E[n/C' + T(1 + n/C')](r/b)^n - \mathscr{E}'. \tag{44}$$

It is possible for the flow not to enter or leave the boundary layer even when $n \neq 0$. This requires $\psi' = 0$ when $r = b$, and

$$\frac{\mathscr{E}'_{\text{rim}}}{\bar{\mathscr{E}}'} = \frac{n/C' + (1 + n/C')T}{(1 + n/C')(1+T) - bT/na}. \tag{45}$$

For the fluid to be at rest throughout the core we also need $\nabla^2\mathscr{E} = 0$, i.e. $\mathscr{E}' \propto r^n$ at $z = \pm a$. If instead $\mathscr{E}'_{\text{rim}} = \bar{\mathscr{E}}'$ (as for instance when $\mathscr{E}$ is independent of z on the curved walls) then $B\psi'_{\text{rim}} = (bT/na - 1)E$, which cannot be zero, and core flow must enter and leave the layer, as it does also when $\bar{\mathscr{E}}' = 0$ and $B\psi' = -\mathscr{E}'$ (the current-free case).

The high-speed flow in the layer is given by (18) and (12). Q_s can be made zero everywhere by a suitable choice of $\mathscr{E}'$ on the curved walls, namely

$$\mathscr{E}' = E((1 + n/c')(1+T) - \cosh(nz/b)/\cosh(na/b)), \tag{46}$$

but Q_z is zero everywhere only for the $n = 0$ harmonic or if $Q_s = 0$.

The case $n = 1$ deserves some attention. The core current is rectilinear, uniform and normal to $\mathbf{B}$. Even though $\mathbf{j} \times \mathbf{B}$ is irrotational there can be fluid motion.

A simple example is that where $\mathscr{E} = kx$ on *all* walls, the current flows in the x-direction and the core moves with uniform velocity

$$v_y = \frac{(k/B)(1 - bT/a)}{(1 + 1/C')(1 + T) - bT/a}, \qquad (T = \tanh a/b), \quad (47)$$

out of and into the boundary layer. Meanwhile the flow in the layer is given by

$$BQ_s = E\cos\theta\left(\frac{\cosh(z/b)}{\cosh(a/b)} - 1\right)$$

$$\text{and } BQ_z = E\sin\theta\left(\frac{\sinh(z/b)}{\cosh(a/b)} - \frac{zT}{a}\right) \quad (48)$$

in which $E = kb/((1 + 1/C')(1 + T) - bT/a)$. Fluid that moves straight across the core returns in the layer on a curved path that takes it nearer to the plane $z = 0$. There is a big difference from the case of a sphere [2] with $\mathscr{E} = kx$, for which no motion occurs. The thermoelectric 'pumping' tendency of the x-wise $\mathscr{E}$-gradient is wholly blocked by the walls in the sphere, but only partially so in the cylinder, in which the fluid velocity reaches a value less than k/B, the velocity at which $\mathbf{v} \times \mathbf{B}$ and Seebeck emf's would balance. This velocity would be reached if $\mathscr{E} = kx$ on the side walls but $\bar{\mathscr{E}} = 0$ on the curved walls. If instead $\mathscr{E} = kx$ on the side walls but (45) is satisfied by $\mathscr{E}$ on the curved walls, there is no core motion.

4.2. *$\mathscr{E}$ Odd in z*

From (21) U' is proportional to $\sinh nz/b$ and (11) leads to the condition at $r = b$:

$$V' + \frac{bT}{n}\frac{dV'}{dr} = 0 \quad \text{or} \quad V' + \frac{a\,dV'}{dr} = 0 \ (n = 0). \quad (49)$$

Equation (20) becomes

$$\frac{d^2V'}{dr^2} + \frac{1}{r}\frac{dV'}{dr} - \left(\frac{C}{a^2} + \frac{n^2}{r^2}\right)V' = \frac{C}{a^2}\mathscr{E}'. \quad (50)$$

The curved wall is a core streamline only if $n = 0$ or $V' + \mathscr{E}' = 0$ at the rim; otherwise the core flow enters and leaves the layers. Equations (49) and (50) show that V and hence W and ψ are determined purely by $\mathscr{E}$ at the walls $z = \pm a$. $\mathscr{E}$ on the curved walls affects only the layers there. $\mathscr{E}'$ at $z = a$ may be expanded as a Fourier series of J_n terms and solutions readily deduced in terms of J_n and I_n. However, some simpler solutions exist.

The analogue of (33) is that where, at $z = a$,

$$\mathscr{E}' = A\{a^2(m^2 - n^2)r^{m-2} - Cr^m + Cr^n b^{m-n}(1 + mT/n)/(1 + T)\} \quad (51)$$

for which, in the core

$$-B\psi = W = A(m^2 - n^2)azr^{m-2}\cos n\theta. \quad (52)$$

To avoid singular z-wise vorticity at $r = 0$ requires $m \geqslant 4$ unless $m = n + 2$. Taking $m = n$ is nugatory. The axisymmetric case ($n = 0$) corresponds *either* to a core with swirl proportional to $z(m \geqslant 4)$ *or* to a stationary core ($m = 2$), the only $\mathscr{E}$-odd situation in which ψ is independent of r and θ and j_z is uniform. If $n = 0$ and $m = 4$ there is uniform angular velocity at each z. The case $n = 1$, $m = 3$ is interesting, for then

$$-B\psi = 8Aazx$$

and the core motion is purely in the y-direction, another rectilinear motion into and out of the boundary layer. If $\mathscr{E}$ on the curved walls is such that $Q_s = 0$ the complete streamlines are all rectangular in planes $x = \text{const}$.

Whenever $\nabla^2\mathscr{E} = 0$ at $z = \pm a$ (i.e. $\mathscr{E}' = Ar^n$) the solution is a relatively simple analogue of (30) and (31), with W proportional merely to $zI_n(cr)$. In the axisymmetric case ($n = 0$) where $\mathscr{E}$ is constant on each wall $z = \pm a$,

$$-B\psi = W = \frac{(z/a)\mathscr{E}I_0(cr)}{I_0(cb) + acI_1(cb)} \quad (53)$$

$\mathscr{E}$ being here the value at $z = a$. Now j_z increases with r like I_0 and the swirl velocity is proportional to I_1. This case includes the case where $\mathscr{E} = kz$ on *all* walls, which should be contrasted with the same case for a spherical container [2], where no motion occurs. Taking $n = 1$, $\mathscr{E} = Ax$ at $z = a$, leads to

$$-B\psi = W = \frac{(z/a)Ab(1 + T)I_1(cr)\cos\theta}{(1 - T)I_1(cb) + cbTI_0(cb)}, \qquad (T = \tanh(a/b)). \quad (54)$$

Again there is motion across the core, into and out of the layers, but it is not now rectilinear. There is a considerable difference from the equivalent spherical case [2] with $\mathscr{E} = Axz/a$, say, in which there is solid body rotation about the x axis. In the cylinder, if $\mathscr{E}$ on the curved walls is such that $Q_s = 0$, the motion still consists of deformed circulation loops centred on the x axis, however.

As regards the boundary layers, when $n = 0$ there is no high speed flow if $\mathscr{E}$ on the curved wall is proportional to z, like U and W. When $n \neq 0$, $Q_s = 0$ only if $\mathscr{E}$ on the curved walls is such that

$$\mathscr{E}' = V'_{\text{rim}}\left(\frac{z}{a} - \frac{\sinh(nz/b)}{\sinh(na/b)}\right) + \frac{z}{a}\mathscr{E}'_{\text{rim}}. \quad (55)$$

Departures of $\mathscr{E}$ from (55) lead merely to extra fluid circulations in the boundary layers which do not upset the core.

5. RECTANGULAR PARALLELEPIPED CONTAINERS

To provide insight into any extra characteristics of TEMHD that arise when the container has sharp edges parallel to the field, we consider the case of a cube of side $2a$. As convenient analytic solutions do not appear to be available, the cube is chosen because its many symmetries greatly facilitate a numerical treatment by the relaxation method. Figure 3(a) shows the

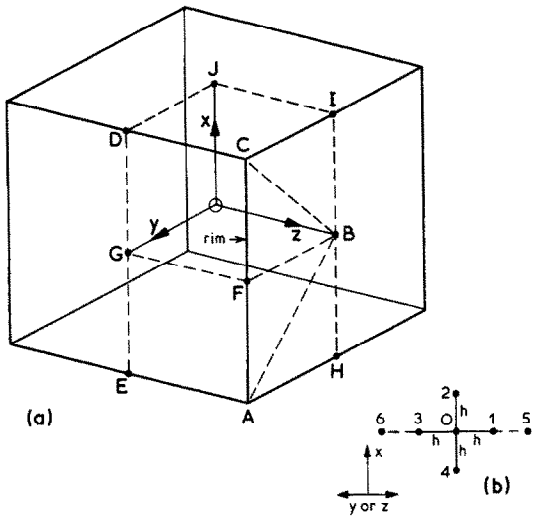

FIG. 3. (a) TEMHD in a cubical container. (b) Relaxation star.

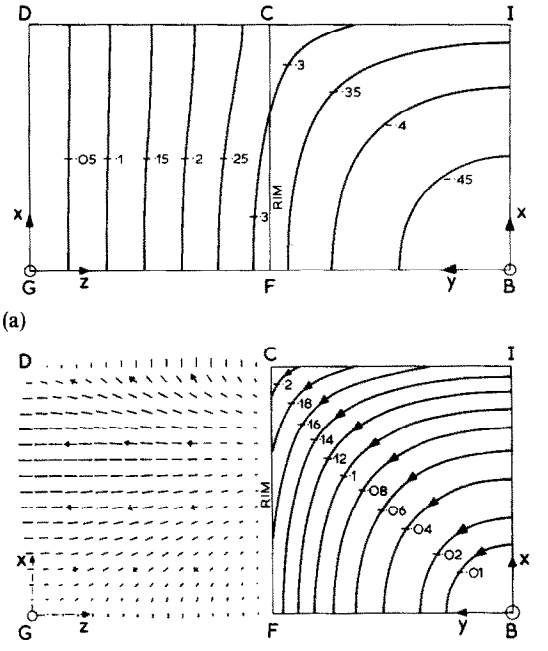

FIG. 4. Cubical container with $\mathscr{E} = kz$, $C = 1.0$: (a) Distribution of U and V in the walls ('flattened'). Contours are labelled with values of $(U \text{ or } V)/ka$. Wall current is normal to these. (b) Fluid motion: core streamlines shown within BICF are labelled with values of $B\psi/kz$. The associated boundary layer flow vectors within CDGF have components proportional to Q_z and Q_x.

axes chosen and the domains over which the equations are to be solved. The cases treated here are those where $\mathscr{E}$ at all walls is linear in either z or in x and/or y, but the method could easily be extended. A square mesh of points with a step-size h equal to a/m, where m is a power of 2, is employed.

5.1. $\mathscr{E}$ *Odd in* z

Provided $\mathscr{E}$ also has symmetry in the planes OBFG and OBCD, it is necessary only to solve for V, ψ over the triangle BCF and for U, Q_s, Q_z over the square CDGF. The case solved here is that where $\mathscr{E} = kz$ at all walls and U and V are treated as one variable V, obeying different differential equations in different places. In terms of the relaxation star of points shown in Fig. 3(b), the improved value of V at the centre is given from (20) and (21) by

$$V_0 = \frac{\Sigma V - \alpha ka}{4 + \alpha}, \tag{56}$$

in which ΣV equals $(V + V_2 + V_3 + V_4)$ and $\alpha = 0$ in CDGF, $C(h/a)^2$ within BCF and $\frac{1}{2}C(h/a)^2$ along CF. The latter is arrived at by first treating 1 as an extrapolated dummy at the rim of CDGF or 3 as such at the rim of BCF and then satisfying (11) by making $V_1 - V_3$ equal in the two cases. An alternative approach equating normal V gradients using a parabolic approximation based on points 6,3,0 and 0,1,5 is found to give indistinguishable results and to be somewhat slower. An extension of the dummy concept, using the symmetries, leads to

$$V_0 = \frac{2V_4 + V_3 - \alpha ka}{3 + \alpha} \tag{57}$$

with $\alpha = 1/4C(h/a)^2$ at the corner C. Relaxations along BC, CD and GFB involve the symmetry about these lines, and V is kept zero along GD. An over-relaxation factor of 1.6 or 1.7 is convenient, and the step-size is halved progressively until $m = 32$, relaxation finally being to within a tolerance of 10^{-6}. Values in the triangle BCI follow from symmetry, and $-W$ and $B\psi$ follow from $-(V + \mathscr{E})z/a$. $Q_x(= -Q_s)$ and Q_z are found from (10) and (12) with $G = 0$.

Figure 4 shows the results for the case $C = 1.0$, drawn with GHOST routines. The right side of Fig. 4(b) shows that, although most of the core motion is an unimpeded vortex motion about the z-axis, the outer core streamlines hit the wall and the flow returns in the boundary layer in the complicated way shown by the left side of the figure. The return flow is mostly across the plane $z = 0$, followed by motion backwards in the core at negative z, but some flow in the layer carries on to negative x, while some circulates backwards via the edge CD. How happily a high speed boundary layer goes round the right angle bend at CD is a matter that deserves experimental scrutiny. To show the influence of C some salient values of V, ψ and Q are given in Table 1, Q being $(Q_x^2 + Q_z^2)^{1/2}$, and ψ being zero at B.

The main effect of raising C is a strengthening of the flow in both core and boundary layer as the potential drops in the walls $z = \pm a$ become more important. When $C = 0$ (perfectly conducting walls) $B\psi + \mathscr{E} =$ const at $z = a$, and so there is no motion in this case, where $\mathscr{E}$ is constant at $z = \pm a$.

The comparison with the other solved cases where $\mathscr{E} = kz$ is instructive. In a sphere [2] or a long, blocked, circular duct [1] there are no boundary layer effects and no motion. In the cube the y-wise core motion

Table 1.

C	$-V/ka$ at B	$-V/ka$ at F	$-V/ka$ at C	$-B\psi/kz$ at C	BQ_{max}/ka	at $z=0$ and $x/a=$
0.2	0.14228	0.09447	0.07771	0.06457	0.00678	0.625
1.0	0.47875	0.32421	0.26912	0.20963	0.02218	0.6875
5.0	0.87958	0.63987	0.54890	0.33068	0.03639	0.6875

across the centre plane $y = 0$ (OBIJ) is not unlike the corresponding motion described by (30) in a long square duct, but the weak boundary layer motion across IJ (compare GF) in the cube has no parallel in the duct, for which $Q_y = 0$ if $\mathscr{E} = kz$, by (25). The cube case gives some indication as to how the rectilinear flow in a long duct would be bent round near and by flat conducting end walls. This turning round would occupy a length of order a, not of order $a/M^{1/2}$, as might have been expected. In the circular cylinder, coaxial with the magnetic field, the core motion across the plane $y = 0$, determined by (53) when $\mathscr{E} = kz$, with v_y proportional to $zI_1(cx)$, is very similar to the cube and duct cases, and there is no high speed boundary layer here, just as in the duct. The biggest contrast occurs with the case of the flat-ended cylinder [3] with its axis in the y-direction, normal to the magnetic field for which there are no high speed boundary layers and there is swirl about the y-axis instead. This is possible because now v_z is not zero. The core motion across the plane $x = 0$ (OBFG) is remarkably similar in the cube and the two cylinder cases, however.

5.2. *$\mathscr{E}$ Even in z*

Provided $\mathscr{E}$ also has symmetry in the plane OBCD and antisymmetry in the plane OBAE it is necessary only to solve for V, G, ψ over the triangle ABC and for U, Q_s, Q_z over the rectangle ACDE. The case solved first is that where $\mathscr{E} = \frac{1}{2}k(x + y)$ on all walls, and V (which again includes U) is found by relaxation according to the formulae

$$V_0 = \tfrac{1}{4}(\Sigma V - \alpha), \quad G_0 = \tfrac{1}{4}\Sigma G, \tag{58}$$

with $\alpha = 0$ within ABC by (13), $\alpha = (Ch^2/a)(\partial G/\partial y)_{rim}$ within ACDE by (14) or half this value along AC, by arguments similar to those used in Section 5.1. At the corner C the formula becomes

$$V_0 = \tfrac{1}{3}(2V_4 + V_3 - (\tfrac{1}{2}Ch^2/a)(\partial G/\partial x)_{rim}). \tag{59}$$

The gradients of G are found from 3 adjacent points by a parabolic approximation. The boundary conditions express the symmetry of V about BC, CD and DE, the symmetry of G about BC, the values $V = G = 0$ along BAE and the value

$$G = \bar{U} + \tfrac{1}{2}k(x + a) \tag{60}$$

along AC, from (16). The method involves iterative relaxations between G and V (or U), $\bar{U}$ derived by Simpson's rule being fed back into the G boundary condition (60) and the G-gradients being fed back into the V-relations (58) and (59). Reasonably stable convergence is achieved by complete relaxation and feedback on each line of points (x = constant) before moving to a new line, and then repeating over the whole domain until relaxation ceases to be necessary within a certain tolerance, progressively lowering this to 10^{-6} when m is raised finally to 32. There is still much scope for improving the numerical method, however. To show core current in $x - y$ planes a stream function H equal to $-\int(\partial G/\partial y)\mathrm{d}x$, is introduced, taking $H = 0$ along BC, while the core flow is revealed by $B\psi$, found from (17), and the boundary layer flows Q_x (i.e. $-Q_s$) and Q_z are found from (8) and (12) in the forms

$$BQ_x = U_{rim} - U$$

$$\text{and } Q_z = -\int_0^z \frac{\partial Q_x}{\partial x}\mathrm{d}z - z\frac{\partial \psi_{rim}}{\partial x}. \tag{61}$$

The values in the triangles BCI and ABH are found by reflections.

Solutions for the case $\mathscr{E} = kx$, regarded as the superposition of the case above and the comparable case $\mathscr{E} = \frac{1}{2}k(x - y)$ are readily computed, and the results presented in Fig. 5 refer to this case, for $C = 1.0$. Figure 5(c) shows how the flow across the centre-plane OBIJ and the equal returning boundary layer flow across JI, also characteristic of the long blocked rectangular duct (see Section 3.3) exchange fluid at and near the end wall CDGF. Most of the flow bends and hits the top wall CDJI and turns sharply back in the fast layer there, rather than proceeding to the end itself where the boundary layer is much slower. In the layers

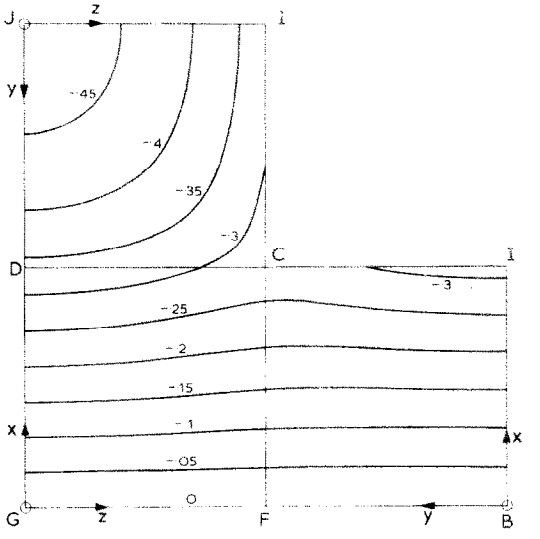

(a) FIG. 5(a).

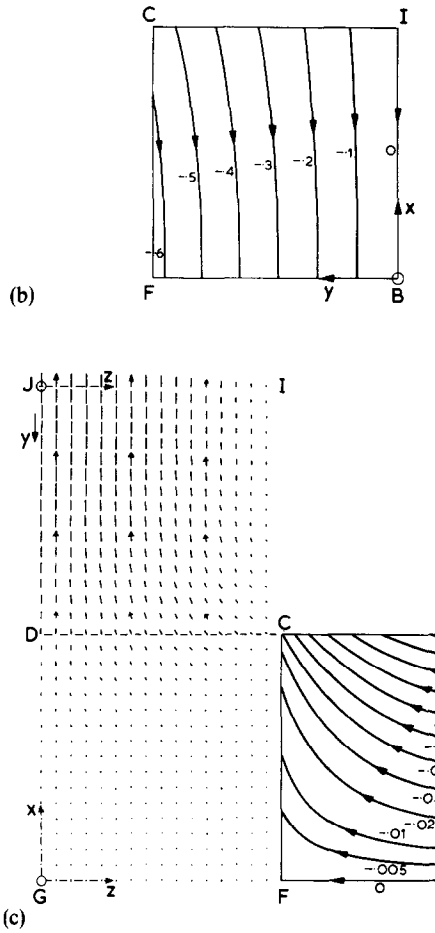

FIG. 5. Cubical container with $\mathscr{E} = kx$, $C = 1.0$: (a) Distribution of U and V in the walls ('flattened'). CI appears twice. Contours are labelled with values of (U or V)/ka. Wall current is normal to these. (b) Core current: current lines are labelled with values of H/ka. (c) Fluid motion: core streamlines shown within BICF are labelled with values of $B\psi/ka$. The associated boundary layer flow vectors are shown to a uniform scale within GFIJ ('flattened'). CI appears twice.

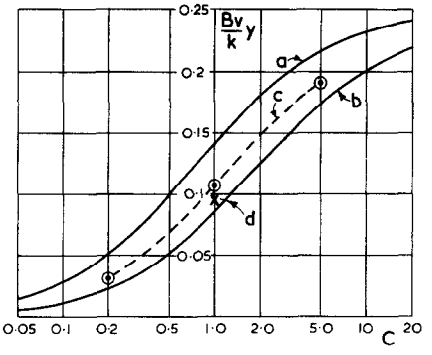

FIG. 6. $\mathscr{E} = kx$ cases. Core velocity at various C. Curve (a): long blocked square duct ($Bv_y = k/(4 + 3/C)$). Curve (b): cylinder coaxial with **B** (case $a = b$) ($Bv_y = k/(4.2 + 7.4/C)$). Curve (c): cube (average velocity across plane $y = 0$). Point (d): cylinder with axis in x-direction (case where semi-length/radius $= \pi/2$) (average velocity across plane $y = 0$).

the fluid returns somewhat closer to the plane $z = 0$ than in the core, because ψ in the core is independent of z but Q_x in the layers is greatest at $z = 0$. The maximum boundary layer flow is at J. The fast flow in the layer round the corner CD is now oblique. To show the influence of C some salient values of V, ψ and Q are given in Table 2. Again larger values of C imply stronger motions in the core and layer. When $C = 0$ (perfectly conducting walls) there is no motion but a uniform core current.

A comparison of the various solved cases for which $\mathscr{E} = kx$ is worthwhile. In a sphere [2] or long blocked circular duct [1] there are no boundary layer effects and no motion. In all the other cases where there are walls parallel to the field at or near the top and bottom (high and low x) there is uniform (or nearly uniform) y-wise motion in the core across the centre-plane $y = 0$, and a return flow in layers at the top and bottom. These cases include the cube, the blocked retangular duct, the flat-ended, circular cylinder coaxial with the field **B** and the cylinder with its axis in the x-direction [3]. The misfit is the cylinder with its axis in the y-direction [3], where the core flow includes a weak closed circulation and the high-speed boundary layers can occur only on walls $y =$ constant, feeding only the core close by. For the other cases, Fig. 6 makes a comparison of the y-wise velocities deduced from Section 3.3, equation (47), Table 2 and reference [3], as C varies. The progression is in line with physical expectation.

The cube case $\mathscr{E} = \frac{1}{2}k(x + y)$ has some interesting features. As Fig. 7 shows, the motion is surprisingly complicated, for all the values of C tested. Although most of the core flow travels in the general direction BA, returning past the corner CD, some of it shortcircuits the corner via the core, above the stagnation region X, while some fluid circulates up and down at and near the wall (see $B\psi/ka = -0.05$).

6. CONCLUDING REMARKS

This paper's main aim has been to show how profoundly TEMHD motions are changed when there are extended areas of wall parallel to the magnetic

Table 2.

C	$-V/ka$ at D	$-V/ka$ at J	$-V/ka$ at C	$-V/ka$ at I	$-B\psi/ka$ at C	$-B\psi/ka$ at I	BQ_{max}/ka
0.2	0.09447	0.14042	0.07737	0.09294	0.01080	0.03221	0.04748
1.0	0.33745	0.47432	0.27545	0.31649	0.03940	0.10689	0.15784
5.0	0.71126	0.88286	0.57476	0.59776	0.08830	0.19245	0.28510

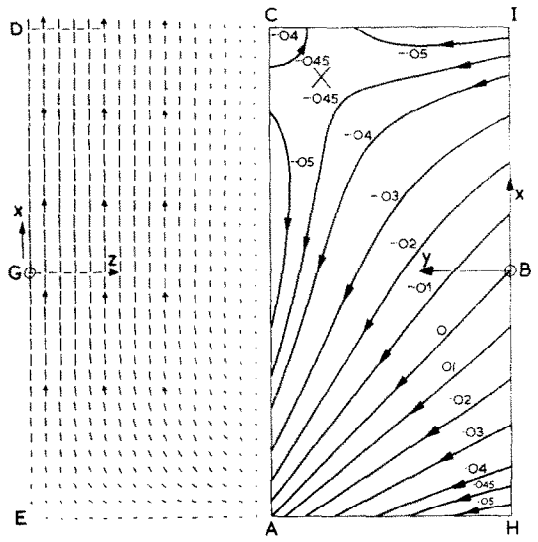

FIG. 7. Cubical container with $\mathscr{E} = \frac{1}{2}k(x + y)$, $C = 1.0$. Fluid motion. Core streamlines shown within AHIC are labelled with values of $B\psi/ka$. The associated boundary layer flow vectors are shown to a uniform scale within ACDE. $BQ_{max}/ka = 0.08043$ at $z = 0$, $x/a = 0.25$.

field. The high speed flows which often occur near these walls could have severe effects on the heat transfer needed to sustain a given interfacial temperature distribution, or on the temperature distribution for a given array of external or internal heat sinks or sources (such as heat release by neutron bombardment). The paper has shown how, for a variety of geometries, the MHD aspect of the problem can be mastered (granted the conditions that allow the inviscid, inertia-free model to be used) thereby opening the way to attacking problems where the heat convection has to be calculated. These are much more challenging, especially where the interface temperature is not known *ab initio*, but is determined by the heat convection, or when, in view of thermal lags and nonlinearity of the convection process, it is not even certain that the combined heat and fluid flow will be steady rather than oscillatory. One particular difficulty is that the odd or even solutions may intermingle when heat convection is introduced.

REFERENCES

1. J. A. Shercliff, Thermoelectric magnetohydrodynamics, *J. Fluid Mech.* **91**, 231–251 (1979).
2. J. A. Shercliff, Thermoelectric magnetohydrodynamics in closed containers, *Physics Fluids* **22**, 635–640 (1979).
3. J. A. Shercliff, The pipe end problem in thermoelectric MHD, *Z. Angew. Math. Phys.* **31**, 94–112 (1980).
4. J. C. R. Hunt, Magnetohydrodynamic flow in rectangular ducts, *J. Fluid Mech.* **21**, 577–590 (1965).

MHD THERMOELECTRIQUE AVEC DES PAROIS PARALLELES AU CHAMP MAGNETIQUE

Résumé—Un métal liquide entre des parois métalliques sous un champ magnétique est brassé thermoélectriquement si la température interfaciale n'est pas uniforme. Quand il y a des zones d'interface parallèle au champ magnétique uniforme, apparaissent des couches limites rapides qui échangent du fluide avec la région centrale. En dehors de ces couches limites, la viscosité et l'inertie peuvent être négligées si le champ magnétique est intense. On considère les mouvements dans des longues conduites de section rectangulaire, des cylindres fermés coaxiaux avec le champ et des conteneurs cubiques. Lorsque la température interfaciale est supposée connue *ab initio*, les effets intenses de la convection thermique ne sont pas explorés.

THERMOELEKTRISCHE MAGNETOHYDRODYNAMIK BEI ZUM MAGNETISCHEN FELD PARALLELEN WÄNDEN

Zusammenfassung—Flüssiges Metall wird zwischen metallischen Wänden unter dem Einfluß eines magnetischen Feldes thermoelektrisch gerührt, wenn die Grenzflächentemperatur nicht gleichförmig ist. Wenn Grenzflächen parallel zum magnetischen Feld vorhanden sind, treten Grenzschichten mit hoher Geschwindigkeit auf, die Flüssigkeit mit der zentralen Region austauschen. Außerhalb dieser Grenzschichten können Zähigkeit und Trägheit vernachlässigt werden, wenn das magnetische Feld stark ist. Bewegungen in langen Kanälen mit rechteckigem Querschnitt, geschlossenen Zylindern, die koaxial zum Feld orientiert sind, und kubischen Behältern werden untersucht. Da angenommen wird, daß die Grenzflächentemperatur von Anfang an bekannt ist, wird der starke Einfluß der konvektiven Wärmeübertragung nicht untersucht.

ТЕРМОЭЛЕКТРИЧЕСКАЯ МАГНИТОГИДРОДИНАМИКА ПРИ НАЛОЖЕНИИ МАГНИТНОГО ПОЛЯ ПАРАЛЛЕЛЬНО СТЕНКАМ

Аннотация — Жидкий металл в объеме, ограниченном металлическими стенками, к которым приложено магнитное поле, перемешивается под действием термоэлектрических сил, если температура на границе раздела фаз неоднородна. Когда граница раздела параллельна постоянному магнитному полю, возникают пограничные слои, способствующие массообмену с центральной областью. При сильном магнитном поле вязкостью и инерцией за пределами этих слоев можно пренебречь. Исследования проводились в удлиненных каналах прямоугольного сечения, замкнутых цилиндрах с соосно направленным полем и кубических резервуарах. Ввиду того, что температура границы раздела считается величиной известной, влияние тепловой конвекции на массообмен не исследовалось.